

Effects of Molecular Composition and Chain
Length on the Interfacial and Thermodynamic
Properties of Cyclic and Linear Polymer Blends

Oluwatumininu E. Ayo-Ojo^a
220052876@stu.ukzn.ac.za
oluwatumininuayoojo@gmail.com

Nkosinathi Dlamini^a
dlaminin2@ukzn.ac.za

^aSchool of Chemistry & Physics, University of KwaZulu-Natal,
Scottsville, Pietermaritzburg, Private Bag X01, 3209, South Africa

CORRESPONDING AUTHOR INFORMATION:

Email: oluwatumininuayoojo@gmail.com;
220052876@stu.ukzn.ac.za

Address: School of Chemistry & Physics, University of
KwaZulu-Natal, Scottsville, Pietermaritzburg,
Private Bag X01, 3209, South Africa

June 9, 2025

Abstract

This research paper comprehensively explores the effects of molecular weight and chain architecture on the interfacial and thermodynamic properties of cyclic and linear polymer blends. Utilizing the Kremer-Grest bead-spring model, the study meticulously investigates how these polymers behave at the polymer-wall interface, with a specific emphasis on their adsorption characteristics and thermal attributes. By showing the heat capacity and thermal stability of polymeric fluids, the research not only advances the understanding of these critical factors within polymer systems but also highlights the broader environmental implications associated with polymer degradation.

The study examines the intricate interaction between molecular design parameters and functionality, revealing how variations in polymer architecture can lead to significant changes in performance and stability. Furthermore, it examines the potential for enhancing the lifecycle performance of polymers, with an eye toward the development of more sustainable materials capable of minimizing environmental impact. Through this exploration, it aims to provide valuable insights that contribute to the ongoing discourse on the optimization of polymer formulations for a greener future, setting the stage for innovations in material science aimed at sustainable applications.

The insights gained from this investigation have the potential to inform future research directions and material design strategies, ultimately supporting the creation of polymers that not only perform effectively but are also environmentally friendly. By integrating a thorough understanding of these relationships, this work aspires to lay the groundwork for the evolution of polymer science, encouraging advancements that align with both technological needs and ecological stewardship.

Keywords: Polymer Blends; Surface Tension; Molecular Dynamics; Chain Architecture; Interface; Thermodynamics.

Introduction

The potential to tweak the surface properties of materials by using polymers with unique topological structures has always stirred up interest in understanding the mechanisms behind surface segregation. This is because topology has been known to strongly influence the structural and dynamic characteristics of polymer systems[1]. It has prompted extensive research into how the repetitive chemical units in polymer chains impact interface diffusion. Research about this often inquires about polymer blends composed of chains with identical chemical compositions but varying molecular architectures, such as linear and cyclic forms. Nevertheless, a thorough understanding of how molecular weight and chain architecture determine preferential adsorption at interfaces remains limited [2].

In the case of linear and cyclic polymer blends, investigations from the self-consistent field (SCF) theory suggest that cyclic polymers will accumulate more at interfaces [3], regardless of their molecular weight, but experimental observations have contradicted this theoretical expectation [4]. An electron spectroscopy for chemical analysis (ESCA) was utilized to examine blends of linear and cyclic polystyrene. The results revealed that linear chains enrich the surface when cyclic chains are present but at low concentrations [5]. This shows the inconsistency for non-freely Jointed Chain polymer conformations, especially in shorter chains when studied experimentally.

The environmental impact of synthetic polymers has become a growing concern, mainly due to their contribution to plastic pollution. While not all polymers are biodegradable, recent research has highlighted the potential for enzymatic degradation of certain polymers [6, 7, 8]. Identifying and designing enzymes that break down polymers into reusable constituents is a promising step toward sustainability. Ideally, this approach would only enable polymers to degrade into their original building blocks, allowing for their reuse in synthesising new materials, achieving a truly circular lifecycle [9]. Achieving this goal, however, requires a deeper understanding of the interfacial and stress-related properties of polymers with varying structures. These properties are key to optimizing polymer blends for performance and degradability, providing knowledge into how polymers, with regard to their architecture, interact with surfaces and respond to environmental stressors.

One prominent area requiring further exploration is the role of polymer structures in determining specific heat capacity values. Established methods address the heat capacities of well-defined polymer structures, but complexities arise when modular architectures like block copolymers or amphiphilic polymers are considered. Further understanding these mechanisms could re-

fine predictions of heat capacity in more complex polymer systems, allowing for improved materials design.

Moreover, hydration significantly affects the heat capacity properties of polymers, particularly in hydrophilic systems [10] demonstrate how the hydration environment can modify the heat capacity of amphiphilic polytartaramides, underscoring the role of water as a crucial factor in complex mixtures. This observation prompts further investigation into how varying polymeric fluid quantities might influence heat capacity, overall thermal stability, and the structural integrity of polymer matrices.

While considerable progress has been made in exploring the relationship between polymers and heat capacity, notable research gaps persist. A central focus of this study is to understand how polymer structure influences heat capacity and to explain the mechanisms behind this structural effect. Heat capacity plays a key role in thermal degradation processes. The study by Okamura and Mihono indicates that polymers with specific thermal properties can undergo photo-induced degradation effectively when exposed to UV light, as the absorbed thermal energy can accelerate the breakdown of polymer chains [11]. This study implies that materials with lower heat capacities might degrade faster than those with higher capacities, as the thermal energy required to reach degradation thresholds is more readily achieved in low-capacity polymers.

A high energy partitioning ratio, indicative of dominant pairwise interaction energies over bonded interaction energies, suggests a less cohesive polymer structure [12]. This lack of strong inter-chain interactions may predispose the polymer to degradation, as weaker connections can be broken more easily compared to polymers with more robust linked networks. This dynamic allows for a higher likelihood of enzymatic or reactive attack on the polymer chains, as indicated by studies on the behaviour of polymers under varying thermal and chemical conditions

The findings of Vijayalakshmi and Madras indicate a connection between molecular motion and thermal properties related to degradation processes. They found that the thermal degradation of their polymer blends, specifically polyvinyl alcohol (PVA), was associated with local molecular motions reflected in its heat capacity [13]. This thermodynamic behavior can enhance polymer degradability, as more mobile molecular chains may facilitate chemical interactions such as hydrolysis or enzymatic degradation that contribute to breaking down the polymer.

Moreover, studies suggest that degradation processes are often dictated by the polymer's structure and its interactions at the molecular level. For instance, Xu et al. explain that the degradation of polymers typically occurs due to the breaking of long molecular chains, which directly links to properties

such as viscosity that are also influenced by heat capacity [14]. Thus, materials characterized by higher mobility and lower bonding interactions, as indicated by lower energy ratios in energy partitioning plots, should experience degradation more readily because the necessary mechanical and chemical bonds needed for stability are less robust.

This study will explore the behaviours of polymer blends, focusing on how molecular weight and chain architecture, particularly linear and cyclic topologies, govern preferential adsorption near solid interfaces. By examining these factors, the work enhances our understanding of how polymer structure influences key thermal, physical, and stress related properties. This insight is crucial for clarifying the relationship between polymer architecture and degradability, thereby supporting the development of environmentally sustainable materials with improved lifecycle performance.

Models

To investigate the behaviour of cyclic and linear polymers at the polymer/vacuum interface, the Kremer–Grest bead-spring model [15] was employed. This model is known for its adaptability to studying various polymeric systems. Polymers are represented as chains of sequential monomers with uniform mass (m), where each monomer connects to its neighbours to form either cyclic (closed-loop) or linear (open-loop) configurations. The interaction potential for non-bonded monomers is described by the truncated and shifted Lennard-Jones (LJ) potential [16] at $r_c = 2.5\sigma$:

$$E_{\text{LJ}}(r) = \begin{cases} 4\epsilon \left[\left(\frac{\sigma}{r} \right)^{12} - \left(\frac{\sigma}{r} \right)^6 \right] + \epsilon_{\text{LJ}}, & r \leq r_c \\ 0, & r > r_c, \end{cases} \quad (1)$$

where r is the distance between two monomers, ϵ is the depth of the potential well, and ϵ_{LJ} is a constant ensuring continuity of the potential at $r = r_c$.

Bonded monomers interact via the LJ potential, coupled with the finitely extensible nonlinear elastic (FENE) potential [17]:

$$E_f(r) = \begin{cases} -\frac{1}{2}Kr_0^2 \ln \left[1 - \left(\frac{r}{r_0} \right)^2 \right], & r \leq r_0 \\ \infty, & r > r_0, \end{cases} \quad (2)$$

where $r_0 = 1.5\sigma$ is the maximum bond extension, and $K = 30\epsilon/\sigma^2$. Overlap between three consecutive beads is prevented, and monomers experience both Brownian and frictional forces[18].

Simulation Details

Initial configurations were generated by randomly placing cyclic and linear polymers of equal chain lengths within a parallelepiped simulation box. The study considered polymer chains of 10 (10Mers), 20 (20Mers), 40 (40Mers) and 60 (60Mers) monomers each. The concentration of cyclic polymers in the blend (C_0) was varied as 10% (C10) and 90% (C90) for all the chains lengths, calculated as:

$$C_0 = 100 \times \frac{N_c^t}{N_c^t + N_l^t}, \quad (3)$$

where N_c^t and N_l^t represent the total number of cyclic and linear polymer monomers, respectively. For all the composition blends, it all contains 120000 monomers.

The simulations were performed using the LAMMPS package [19], employing a velocity-Verlet algorithm with a timestep of $\Delta t = 0.005\tau$, where $\tau = (m\sigma^2/\epsilon)^{1/2}$ and: m : The mass of a particle (e.g., a polymer bead in the simulation); σ : The characteristic length scale, often the particle diameter or the distance where inter-particle interactions are significant; ϵ : The characteristic energy scale, related to the strength of particle interactions (e.g., the depth of the Lennard-Jones potential well); τ : The time unit in reduced units, derived from the physical parameters m , σ , and ϵ . It represents the time it takes for a particle to traverse a distance on the order of σ under the influence of the energy scale ϵ .

. The systems were initially equilibrated in the NPT ensemble at $P = 0$ and $T = \epsilon/k_B$, where, T : The absolute temperature of the system in reduced units, k_B : Boltzmann's constant, which relates the average kinetic energy of particles to the temperature while using a Langevin thermostat and a Berendsen barostat, with periodic boundary conditions applied along all three directions.

After equilibration, periodicity along the z -axis was removed, and the simulation box was elongated in this direction to have these polymers exposed to nearly equal volumes of a wall interface at both the top and bottom so as to evaluate the influence of the interfacial confinement on the polymers. Simulations were conducted in the presence of walls, as the polymers are expected to interact directly with such interfaces. Incorporating wall boundaries enables a more accurate analysis of polymer behavior under realistic confinement conditions.

Results and Discussion

Local Composition

Local composition refers to the relative proportion of each polymer type in the system in a polymer blend of cyclic and linear polymers [20]. This is typically expressed as a fraction of the number of polymers or monomers.

The composition of cyclic and linear polymers is calculated as:

$$\text{Composition of Cyclic Polymers (\%)} = \frac{N_{\text{cyclic}}}{N_{\text{total}}} \quad (4)$$

$$\text{Composition of Linear Polymers (\%)} = \frac{N_{\text{linear}}}{N_{\text{total}}} \quad (5)$$

Where N_{cyclic} and N_{linear} are the number of atoms (or monomers) belonging to cyclic and linear polymers, respectively, and N_{total} is the total number of atoms in the system.

This calculation was implemented using a Fortran code to parse the LAMMPS output dump file for numbers of the cyclic and linear monomers at the varying compositions indicated above, which will be in the slab of size σ along the z -direction. This analysis of the local composition profiles of cyclic and linear polymer blends exposed to a wall along the Z -axis is shown below. The systems includes the four polymer lengths and two compositions investigated: 10% Cyclic - 90% Linear and 10% Linear - 90% Cyclic.

The wall is located at $Z = 0$, and the bulk region is at $Z = 40$ along the z -axis.

Cyclic Polymers at 10% Composition

The observed behavior of polymer composition near a wall as seen in Figure 1, particularly the depletion of short chains and the enhancement of longer chains, can be explained through a combination of entropic and energetic contributions to their respective configurations. As one approaches the wall ($Z \approx 0$), it has been observed that the concentration of short polymer chains (approximately 10-mers) decreases, while longer chains (e.g., over 20-mers) tend to localize and enhance their concentration in that same region. This phenomenon is attributable to the entropic penalties faced by cyclic polymers, which tend to adopt compact configurations that limit their interactions with the wall [21, 22].

The entropic effects stem from the chains' conformational flexibility; longer cyclic polymers have more degrees of freedom but incur significant entropic costs when constrained in bulk conditions. Thus, when these longer polymers

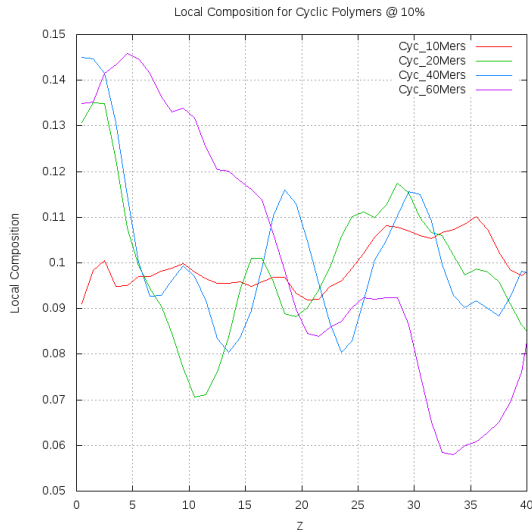


Figure 1: Local composition of cyclic polymers at 10% composition (10Mers, 20Mers, 40Mers, 60Mers).

approach a wall, they are incentivized to localize in order to minimize their entropic penalty, leading to a greater concentration near the interface [21]. Studies corroborate that polymer-wall interactions can effectively draw polymers into the interface, leading to a pronounced alignment parallel to the wall [22]. The attractive interactions between the polymer chains and the wall can promote this aggregation effect, enhancing their effective concentration in the near-wall region.

Cyclic Polymers at 90% Composition

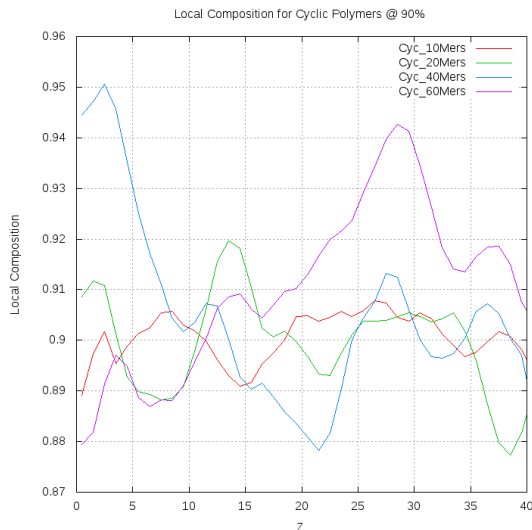


Figure 2: Local composition of cyclic polymers at 90% composition (10Mers, 20Mers, 40Mers, 60Mers).

Furthermore, at lower concentrations of cyclic polymers, where interactions are weaker due to their compact architecture, the differentiation in behavior between short and long chains is even more pronounced. Research indicates that as polymer chain lengths increase, the tendency for these polymers to intercalate and form stable arrangements near the wall becomes stronger due to their spatial configurations and interactions [23]. In contrast, from Figure 2 the bulk region ($Z > 20$) experiences only slight depletion influenced by stronger enhancement near the wall, affirming the dominance of chain length on the spatial distribution of polymers.

The overall density of polymer chains near the wall is influenced not only by their length but also by crowding effects at higher concentrations, where enthalpic interactions further diminish entropic drives, resulting in significant accumulations near the wall [21]. Longer cyclic polymers are particularly adept at forming stable conformations in this region, making them more prone to enhancing the local composition when in a concentrated blend. Comprehensive studies have explicitly illustrated this dynamic and established a clear under-

standing of the interplay between chain length and concentration in relation to wall interactions [22, 24].

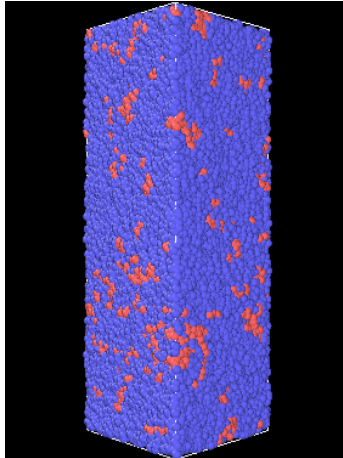


Figure 3: Snapshots of the simulation box for 40 mers at 90% cyclic composition.

In Figure 3, we present a visual representation of the simulation box for a polymer blend comprising 40 mers, specifically consisting of 10% cyclic (Red) and 90% linear polymers (Blue). This image serves to illustrate the typical polymer-substrate(s) that are central to our examination of interfacial properties. Notably, the snapshot confirms the presence of an adequate quantity of both polymer types in proximity to the walls, thereby corroborating the local composition plots discussed previously.

Temperature and Total Energy Calculation

The temperature in molecular dynamics (MD) represents the kinetic energy of the atoms/molecules in the system [25]. The formula is:

$$T = \frac{2K}{3N \cdot k_B} \quad (6)$$

Where, K : Total kinetic energy, N : Number of degrees of freedom, k_B : Boltzmann constant

The total energy is the addition of kinetic energy (K) and potential energy (U):

$$E_{\text{total}} = K + U \quad (7)$$

which represents the overall energy of the system at a given state.

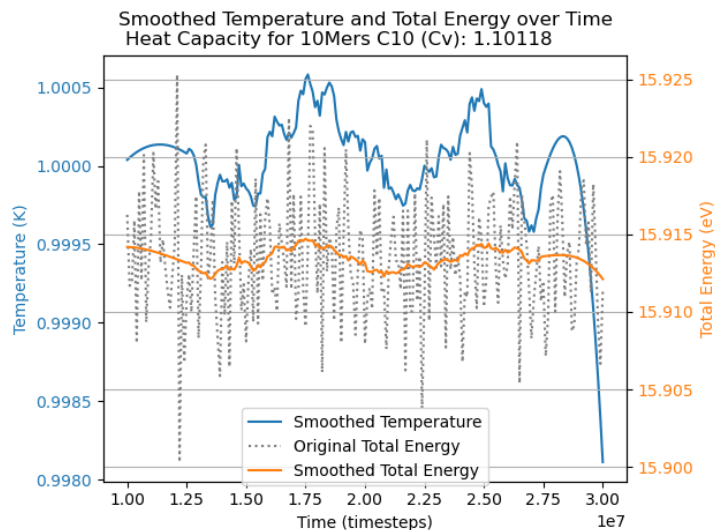
Heat Capacity Calculation

The heat capacity at constant volume (C_v) was calculated using the fluctuation formula derived from statistical mechanics [26]:

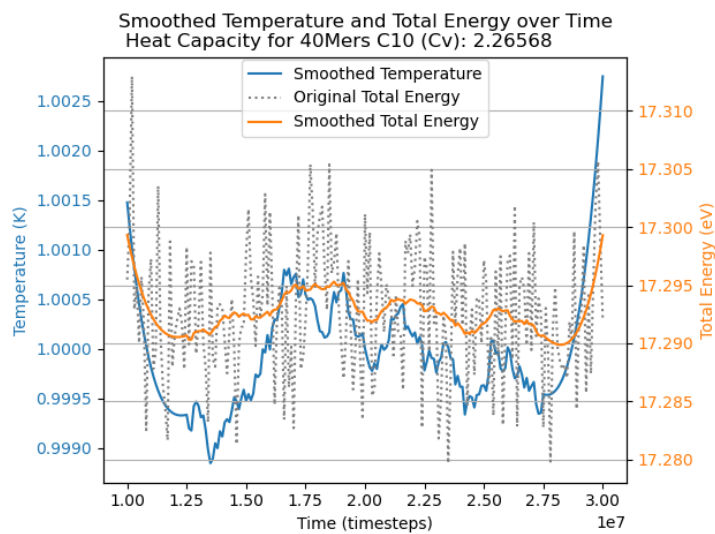
$$C_v = \frac{\langle E^2 \rangle - \langle E \rangle^2}{k_B T^2} \quad (8)$$

Where: E : Total energy, $\langle E \rangle$: Average total energy, $\langle E^2 \rangle$: Mean of the square of total energy, k_B : Boltzmann constant (1.380649×10^{-23} J/K), T : Average temperature.

It helps to measure the blend's ability to store heat at constant volume [27]. It should also indicate energy fluctuations in the system, revealing phase transitions or specific heat behaviours.

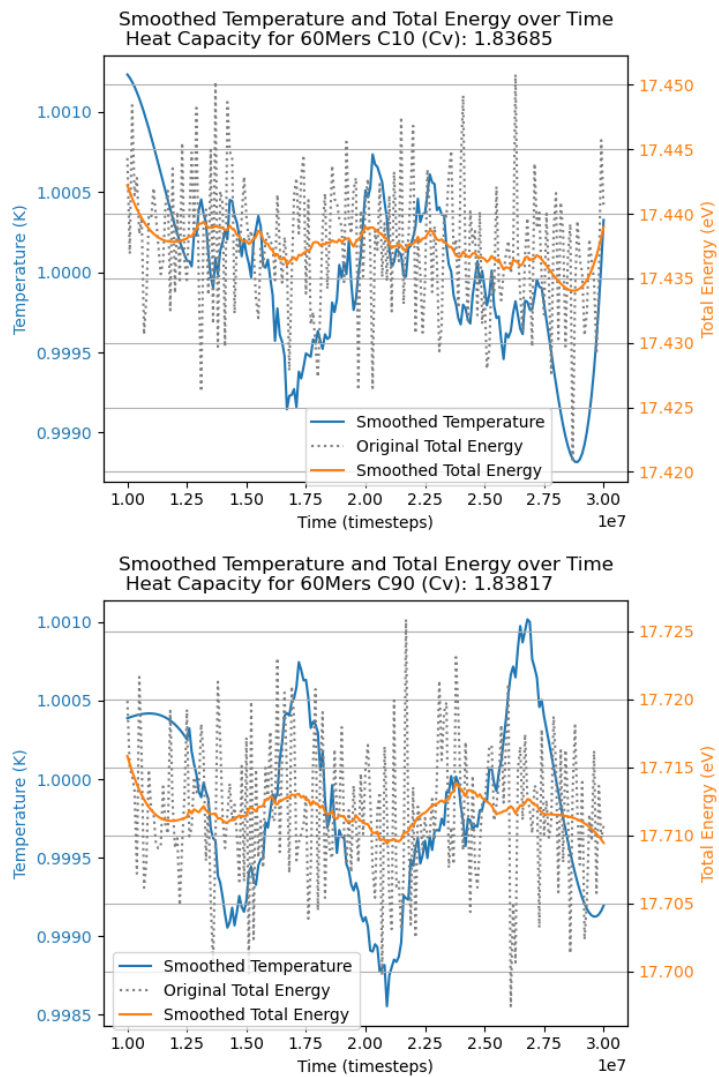


10Mers Polymers



40Mers polymers

Figure 4: Temperature and Total Energy Over Time (Heat Capacity(Cv))



60Mers Polymers

Figure 5: Temperature and Total Energy Over Time (Heat Capacity(Cv))

From Figure 4, 5 the smoothed temperature curves reveal fluctuations around a mean value, indicating how well the polymer system maintains thermal stability over time. The total energy trends reflects the stability of the energy states of the system, which helps to identify thermal equilibrium. After smoothing, the total energy (orange line) appears relatively stable over time. This stability indicates that the system is equilibrated and energy conservation is maintained. Small oscillations in the total energy show the interplay between kinetic and potential energy during the simulation.

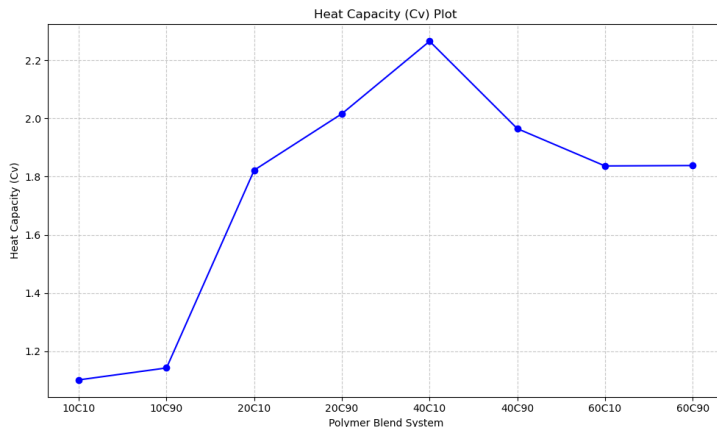


Figure 6: Heat Capacity Plots for the Polymer Blend System

Within the investigation of the heat capacities of polymer systems, particularly those composed of varied blends such as C10 (10% cyclic and 90% linear) versus C90 (90% cyclic and 10% linear), significant discrepancies in temperature and total energy profiles are observed. The differences can be attributed primarily to both the specific compositions and the chain lengths of the polymer blends under consideration. The 10-mers C10 polymer blend demonstrates a higher heat capacity (C_v) than its C90 counterpart, which is supported by previous literature noting similar trends, particularly in the context of polymer thermal responses [28]. This higher C_v suggests that C10 systems can effectively absorb more heat energy before a discernible temperature change occurs, implying enhanced thermal responsiveness.

Notably, the augmented heat capacity for systems featuring a higher proportion of cyclic polymers, particularly in the C90 configuration, can be rationalized through the compact nature of cyclic structures, which exhibit limited

configurational degrees of freedom. These structural characteristics enhance thermal stability, especially in shorter chain configurations, a phenomenon supported by findings in polymer science [29]. As such, the dynamics may become increasingly restricted in longer chains, resulting in varied thermal properties.

For instance, polymers configured with 40 monomer units (40-mers) of C10 are noted to exhibit competitive heat capacities among the various systems examined. This suggests that these polymers might facilitate greater thermal energy absorption due to enhanced intra-chain interactions or augmented configurational freedom [30, 31]. However, experimental literature must specifically address the precise thermal behaviors across differing chain lengths to draw accurate comparisons.

In the scenario involving polymers of 60 monomer units (60-mers), it is important to detail the observed reduction in C_v for the C10 blend relative to C90. This phenomenon may indicate that once the polymer chain length exceeds a certain threshold, approximately beyond its optimal configuration, the dynamic behavior of the chains begins to exhibit constraints, thus affecting their configurational freedom and leading to lower heat capacities. This pattern emphasizes the relationship between chain length and heat capacity, evident across various polymer studies [32], and suggesting a complex interplay rather than a strictly linear correlation.

The comparative analysis of these heat capacities aligns with broader trends in polymer science, indicating that variations in molecular architecture significantly influence thermal properties. Taking into consideration the broader implications of these findings, they resonate with the literature emphasizing the critical role of molecular architecture on the heat capacity of polymers and their propensity for thermal degradation [33, 29]. Understanding the interplay between structure and thermal properties is essential for advancing polymer materials with attuned thermal responses.

Energy Partitioning in the Polymer System

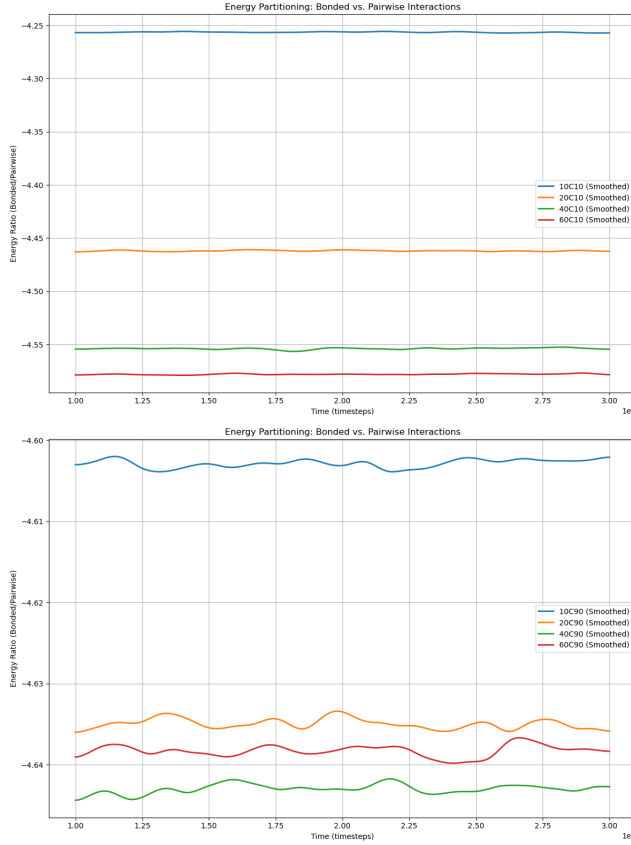


Figure 7: Energy Partitioning (Bonded Vs. Pairwise Interaction)

The characterization of energy partitioning in polymer blends, particularly in systems composed of varying ratios of cyclic and linear polymers, reveals distinct behaviors governed by chain architecture. From Figure 7, it can be seen that the energies remain relatively constant, indicating that the system reached a steady state. As seen here with the negative values, a low energy ratio reflect higher mobility or less structural rigidity in the blend [34]. The energy ratios (bonded/pairwise interactions) are consistently negative, signifying that

the pairwise interaction energies dominate over the bonded interaction energies in all cases. A high energy ratio would have shown that bonded interactions dominate over pairwise interactions. This may suggest strong structural integrity or chain connectivity in the polymer [35]. The blends with 10% cyclic and 90% linear content (C10) compared to those with 90% cyclic and 10% linear content (C90) shows that the former tends to exhibit higher total energy partitioning. This behavior arises from the inherent structural properties of cyclic polymers, whose closed-loop conformations can facilitate enhanced interactions with neighboring chains, thereby contributing more significantly to the overall energy landscape. In contrast, linear polymers predominantly influence the pairwise interaction energy due to their greater conformational flexibility, which enables a wider range of intermolecular contacts [36].

The energetic profile of such polymer systems suggests that configurations with substantial bonded energy contributions typically correspond to more constrained or rigid conformations. Meanwhile, systems dominated by pairwise interaction energies benefit from improved packing efficiency and stronger non-bonded attractions. For instance, in blends like 10C10 (10-mers, C10) and 10C90 (10-mers, C90), the relative energy contributions shift depending on the proportion of cyclic to linear chains. These differences highlight the increasing prominence of pairwise interactions in blends with elevated cyclic content.

Although these trends may extend across different chain lengths, direct empirical data linking chain length to energy partitioning in cyclic and linear polymer systems remains limited. As such, interpretations regarding the energetic behavior of systems at varying chain lengths, particularly those considered here should be made cautiously until further experimental validation becomes available.

As chain length increases, particularly in intermediate regimes such as 20-mers and 40-mers, energy ratios may trend toward more negative values. This behavior could reflect a rise in potential interaction sites that promote intensified pairwise interactions. Due to their compact configurations, cyclic polymers typically exhibit a higher density of contacts, which may encourage greater entanglement and interaction frequency. Nevertheless, firm conclusions regarding these tendencies and their relationship to energy partitioning require further in-depth investigation.

Surface Tension in Polymer Blends

This study investigates the surface tension of polymer blends (γ) comprising cyclic and linear chains under confinement along the Z-axis. Surface tension is the fundamental thermodynamic property that quantifies the energy required

to maintain an interface between two phases [37]. In the context of polymer blends, especially those confined within a wall along the z -axis, surface tension provides critical knowledge of the interfacial properties of the system [38]. In polymer systems, surface tension usually arises due to the imbalance of forces at the interface. This can occur at the boundary between polymers and confining walls or regions with different polymer compositions, but in this case, the boundary between polymers and confining walls is considered.

In scientific terms, surface tension measures the system’s resistance to deformation or disruption at the interface and provides insight into the stability and miscibility of polymer blends [39].

The surface tension from our LAMMPS simulations is derived from the pressure tensor components using the formula:

$$\gamma = \int_{z_{lo}}^{z_{hi}} \left[P_{zz} - \frac{1}{2}(P_{xx} + P_{yy}) \right] dz, \quad (9)$$

Where, P_{zz} : Normal stress component along the z -axis, P_{xx} , P_{yy} : Normal stress components in the x - and y -directions, respectively, z_{lo} and z_{hi} : The bounds of the simulation box along the z -axis.

This formula captures the difference between the pressure acting normal to the interface (P_{zz}) and the average lateral pressure $((P_{xx} + P_{yy})/2)$, integrated across the z -dimension. LAMMPS computes the pressure tensor at every Timestep, which is spatially averaged or binned along the z -axis. The pressure difference $(P_{zz} - (P_{xx} + P_{yy})/2)$ is integrated across the z -direction to obtain surface tension and noise in the raw data is reduced using Savitzky-Golay filter to emphasize significant trends. The blends consist of the varying chain lengths and two distinct compositions we have been working with:

- 10% Cyclic, 90% Linear (denoted as `log_10C10.lammps`)
- 90% Cyclic, 10% Linear (denoted as `log_10C90.lammps`) for the 10 Mers
- 10% Cyclic, 90% Linear (denoted as `log_20C10.lammps`)
- 90% Cyclic, 10% Linear (denoted as `log_20C90.lammps`) for the 20 Mers
- 10% Cyclic, 90% Linear (denoted as `log_40C10.lammps`)
- 90% Cyclic, 10% Linear (denoted as `log_40C90.lammps`) for the 40 Mers
- 10% Cyclic, 90% Linear (denoted as `log_60C10.lammps`)
- 90% Cyclic, 10% Linear (denoted as `log_60C90.lammps`) for the 60 Mers

Surface Tension Plots

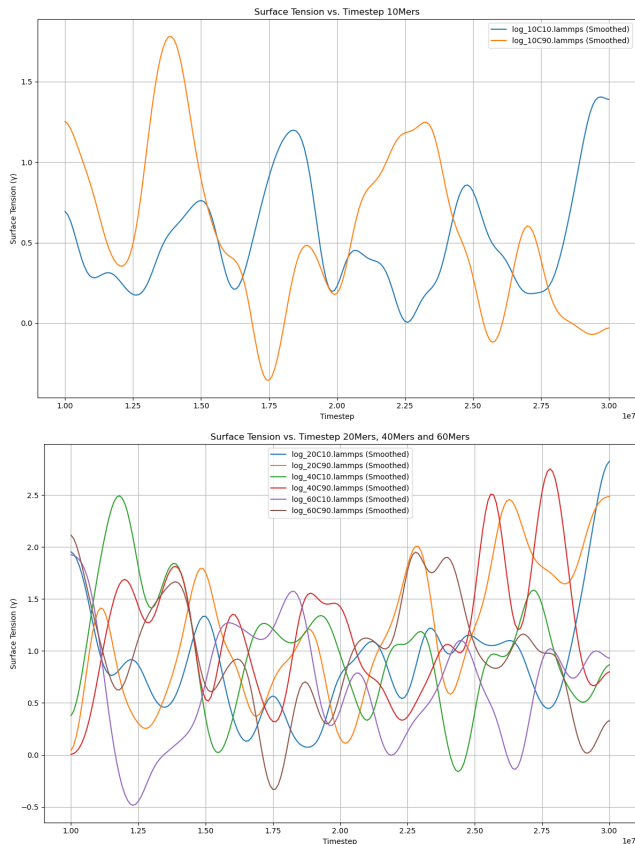


Figure 8: Surface Tension (γ) vs. Timestep for polymer blends of 10-mers under Z-axis confinement. The blue curve corresponds to the 10% Cyclic, 90% Linear composition, while the orange curve represents the 90% Cyclic, 10% Linear composition.

The analysis of surface tension fluctuations in polymer blends reveals distinct oscillatory patterns that stem from differences in molecular composition. Specifically, blends comprising 10% cyclic and 90% linear polymers (C10) and those with 90% cyclic and 10% linear polymers (C90) exhibit notable differ-

ences in both amplitude and frequency of surface tension variations, which can be attributed to their underlying structural features. The C10 blend demonstrates relatively small-amplitude oscillations, indicative of a more stable interfacial configuration. In contrast, the C90 blend displays more pronounced fluctuations, suggesting increased interfacial instability and variability.

This variation in interfacial behavior is largely influenced by the flexibility of linear polymers, which enables more homogeneous packing and reduces interfacial tension due to fewer entropic constraints. Conversely, cyclic polymers, constrained by their closed-loop topology, introduce increased rigidity and result in higher amplitude oscillations in cyclic-rich blends [40]. In such systems, the inability of cyclic polymers to efficiently pack at the interface leads to destabilization, further exacerbated by their restricted conformational freedom [41].

Furthermore, with increasing chain length (e.g., 20-mers, 40-mers, and 60-mers), confinement effects stemming from blend morphology intensify these differences in interfacial behavior. Longer cyclic polymers experience greater entropic limitations, producing higher stress anisotropy and contributing to more significant surface tension fluctuations. This trend aligns with studies demonstrating how dense, tightly packed polymer configurations create localized stress variations and influence interfacial responses [42].

A particularly notable phenomenon is the appearance of negative surface tension values during simulations involving blends with a high concentration of cyclic polymers (such as C90) and long chains (e.g., 60-mers). While counterintuitive, such values may represent transient states or structural rearrangements driven by the system’s attempt to minimize free energy through interactions with confining walls. These behaviors are especially relevant under conditions of extreme confinement, where interfacial properties are governed by complex balances of intermolecular forces [43].

Conclusion

In conclusion, this study demonstrates that the molecular weight and chain architecture of polymers, specifically in the context of linear and cyclic topologies, play a crucial role in their interactions at solid interfaces. The findings indicate that although self-consistent field theory predicts that cyclic polymers will gather more readily at these interfaces, experimental data reveal that linear chains may also enhance surface concentration at lower concentrations. Furthermore, shorter polymers, such as oligomers, exhibit low heat capacity, which could suggest a propensity for accelerated degradation; however, this relation-

ship is not linear. Notably, once a chain length surpasses approximately 40 monomers, the heat capacity begins to decrease, indicating a threshold effect.

Additionally, the analysis shows that shorter polymer chains tend to exhibit the highest energy partitioning, reflecting a dominance of pairwise interactions over bonded interactions. This characteristic implies a less cohesive structure, suggesting that polymers of shorter chains may be more conducive to degradation. Given these insights, it is implied that the design of degradable polymers would benefit from incorporating shorter chain lengths.

Looking forward, the exploration of integrating nano-fillers presents a promising avenue for future research. Such modifications could modulate the thermal properties of the polymers and yield a wider variety of results, allowing for further analysis and optimization of polymer performance.

Acknowledgments

The authors also thank the Centre for High-Performance Computing (CHPC) at CSIR for the generous allocation of computational resources.

Data Availability

The data supporting this study’s findings are available from the corresponding author, O. E. upon reasonable request.

Generative Artificial Intelligence Declaration

I have used Generative AI tools, specifically ChatGPT and Grammarly, to rephrase portions of my writing for clarity and readability

Disclosure of interest

No potential conflict of interest was reported by the author(s).

Funding

This research was partly funded by Erasmus+ Mobility Scholarship through Agreement n. 2022-1-IT02_KA171-HED-000077971.

Author Contributions

Conceptualization, Investigation, Writing—original draft, and Data curation were performed by Oluwatuminu E. Ayo-Ojo. Writing—review and editing for intellectual content, and Visualization were carried out by both Oluwatuminu E. Ayo-Ojo and Nkosinathi Dlamini. Supervision and Project Validation were conducted solely by Nkosinathi Dlamini. All authors have read and agreed to the published version of the manuscript and have accepted to be accountable for all aspects of the work.

References

- [1] W. Hu, T. Chen, K. Terayama, S. Wang, I. Watanabe, and M. Naito. Topological alternation from structurally adaptable to mechanically stable crosslinked polymer. *Science and Technology of Advanced Materials*, 23:66–75, 2022.
- [2] Z. Flint, H. Grannemann, K. Baffour, N. Koti, E. Taylor, E. Grier, C. Sutton, D. Johnson, P. Dandawate, R. Patel, S. Santra, and T. Banerjee. Mechanistic insights behind the self-assembly of human insulin under the influence of surface-engineered gold nanoparticles. *ACS Chemical Neuroscience*, 15:2359–2371, 2024.
- [3] A. Goodson, M. S. Rick, J. E. Troxler, H. S. Ashbaugh, and J. N. L. Albert. Blending linear and cyclic block copolymers to manipulate nanolithographic feature dimensions. *ACS Applied Polymer Materials*, 4:327–337, 2021.
- [4] A. Goodson, M. S. Rick, J. E. Troxler, H. S. Ashbaugh, and J. N. L. Albert. Blending linear and cyclic block copolymers to manipulate nanolithographic feature dimensions. *ACS Applied Polymer Materials*, 4:327–337, 2021.
- [5] G. Pellicane, M. M. Megnidio-Tchoukouegno, G. T. Mola, and M. Tsige. Surface enrichment driven by polymer topology. *Physical Review E*, 93, 2016.
- [6] R. Wei, D. Breite, C. Song, D. Gräsing, T. N. Ploss, P. Hille, R. Schwerdtfeger, J. Matysik, A. Schulze, and W. Zimmermann. Biocatalytic degradation efficiency of postconsumer polyethylene terephthalate packaging determined by their polymer microstructures. *Advanced Science*, 6, 2019.
- [7] F. Kawai, T. Kawabata, and M. Oda. Current knowledge on enzymatic pet degradation and its possible application to waste stream management and other fields. *Applied Microbiology and Biotechnology*, 103:4253–4268, 2019.
- [8] T. B. Thomsen, S. Schubert, C. Hunt, K. Borch, K. Jensen, J. Brask, P. Westh, and A. S. Meyer. Rate response of poly(ethylene terephthalate)-hydrolases to substrate crystallinity: basis for understanding the lag phase. *ChemSusChem*, 16, 2023.

- [9] H. Tran, V. R. Feig, K. Liu, H. Wu, R. Chen, J. Xu, K. Deisseroth, and Z. Bao. Stretchable and fully degradable semiconductors for transient electronics. *ACS Central Science*, 5:1884–1891, 2019.
- [10] Y. Chi, S. Xu, X. Xu, Y. Cao, and J. Dong. Studies of relationship between polymer structure and hydration environment in amphiphilic polytartaramides. *Journal of Polymer Science Part B: Polymer Physics*, 55:138–145, 2016.
- [11] H. Okamura and K. Mihono. Degradation of modified polystyrenes having degradable units by near-infrared light irradiation. *Applied Research*, 3, 2023.
- [12] W. Xu, J. F. Douglas, and X. Xu. Role of cohesive energy in glass formation of polymers with and without bending constraints. *Macromolecules*, 53:9678–9697, 2020.
- [13] S. Vijayalakshmi and G. Madras. Thermal degradation of water soluble polymers and their binary blends. *Journal of Applied Polymer Science*, 101:233–240, 2006.
- [14] X. Xin, G. Yu, Z. Chen, K. Wu, X. Dong, and Z. Zhu. Effect of polymer degradation on polymer flooding in heterogeneous reservoirs. *Polymers*, 10:857, 2018.
- [15] W. B. Lee and K. Kremer. Entangled polymer melts: relation between plateau modulus and stress autocorrelation function. *Macromolecules*, 42:6270–6276, 2009.
- [16] P. Moscato and M. N. Haque. New alternatives to the lennard-jones potential. *Scientific Reports*, 14, 2024.
- [17] F. Serafini, F. Battista, P. Gualtieri, and C. M. Casciola. Kinetic energy budget in turbulent flows of dilute polymer solutions. *Journal of Fluid Mechanics*, 2023.
- [18] S. Yu, R. Chu, G. Wu, and X. Meng. A novel fractional brownian dynamics method for simulating the dynamics of confined bottle-brush polymers in viscoelastic solution. *Polymers*, 16:524, 2024.
- [19] A. Y. Al-Maharma, F. Bamer, and B. Markert. Molecular dynamics study on the effect of interfacial cellulose polymers in strengthening the stress transfer between alumina nanoparticles and epoxy. *Pamm*, 22, 2023.

- [20] R. Gul and W. A. K. Mahmood. Studies on a novel microporous electro-spun poly(vinyl alcohol)-based polymer electrolyte membranes for high-performance battery applications. *Journal of the Chinese Chemical Society*, 70:1972–1985, 2023.
- [21] R. Zhang, B. Lee, C. M. Stafford, J. F. Douglas, A. V. Dobrynin, M. R. Bockstaller, and A. Karim. Entropy-driven segregation of polymer-grafted nanoparticles under confinement. *Proceedings of the National Academy of Sciences*, 114:2462–2467, 2017.
- [22] S. Li, J. Li, M. Ding, and T. Shi. Effects of polymer–wall interactions on entanglements and dynamics of confined polymer films. *The Journal of Physical Chemistry B*, 121:1448–1454, 2017.
- [23] M. R. Smyda and S. C. Harvey. The entropic cost of polymer confinement. *The Journal of Physical Chemistry B*, 116:10928–10934, 2012.
- [24] H. Merlitz, S. Jens-Uwe, X. Cao, and C. Wu. Entropy dominated behaviors of confined polymer—nanoparticle composites. *Chinese Physics B*, 21:118202, 2012.
- [25] J. Zhang, J. Wang, Z. Li, J. Zhu, and B. Lü. Molecular dynamics simulation and gas generation tracking of pyrolysis of bituminous coal. *ACS Omega*, 7:11190–11199, 2022.
- [26] H. C. Öttinger, M. A. Peletier, and A. Montefusco. A framework of nonequilibrium statistical mechanics. i. role and types of fluctuations. *Journal of Non-Equilibrium Thermodynamics*, 46:1–13, 2020.
- [27] H. Yurseven and Z. Unlu. Critical behaviour of the raman frequency shifts in the vicinity of the - phase transition in nh4br. *High Temperature Materials and Processes*, 25:143–148, 2006.
- [28] S. Pal, G. Balasubramanian, and I. K. Puri. Modifying thermal transport in electrically conducting polymers: effects of stretching and combining polymer chains. *The Journal of Chemical Physics*, 136, 2012.
- [29] T. Zhang and T. Luo. Role of chain morphology and stiffness in thermal conductivity of amorphous polymers. *The Journal of Physical Chemistry B*, 120:803–812, 2016.

- [30] Y. Ding, S. I. Stoliarov, and R. Kraemer. Development of a semiglobal reaction mechanism for the thermal decomposition of a polymer containing reactive flame retardants: application to glass-fiber-reinforced polybutylene terephthalate blended with aluminum diethyl phosphinate and melamine polyphosphate. *Polymers*, 10:1137, 2018.
- [31] I. A. Silantyeva and P. N. Vorontsov-Velyaminov. Thermodynamic properties of star shaped polymers investigated with wang-landau monte carlo simulations. *Macromolecular Symposia*, 317-318:267–275, 2012.
- [32] H. Chen. Thermal conductivity of amorphous and crystalline polyethylene: a molecular dynamics study. *Journal of Materials, Processing and Design*, 7, 2023.
- [33] C. Huang, X. Qian, and R. Yang. Thermal conductivity of polymers and polymer nanocomposites. *Materials Science and Engineering: R: Reports*, 132:1–22, 2018.
- [34] W. Jiang, F. Wu, Z. Mei, R. Shi, and D. Xie. Low-grade flow energy harvesting by low-mass-ratio oscillating bent plate. *Energies*, 15:1606, 2022.
- [35] J. Li, Y. Gao, D. Cao, L. Zhang, and Z. Guo. Nanoparticle dispersion and aggregation in polymer nanocomposites: insights from molecular dynamics simulation. *Langmuir*, 27:7926–7933, 2011.
- [36] V. Somsongkul, S. Jamikorn, A. Wongchaisuwat, S. H. Thang, and M. Arunchaiya. Efficiency and stability enhancement of quasi-solid-state dye-sensitized solar cells based on peo composite polymer blend electrolytes. *Advanced Materials Research*, 1131:186–192, 2015.
- [37] A. Lamorgese and R. Mauri. Phase-field modeling of interfacial dynamics in emulsion flows: nonequilibrium surface tension. *International Journal of Multiphase Flow*, 85:164–172, 2016.
- [38] H. Ma. Fundamentals. *Oscillating Heat Pipes*, pages 13–86, 2015.
- [39] K. Bryson, T. I. Löbbling, A. H. E. Müller, T. P. Russell, and R. C. Hayward. Using janus nanoparticles to trap polymer blend morphologies during solvent-evaporation-induced demixing. *Macromolecules*, 48:4220–4227, 2015.

- [40] M. M. Megnidio-Tchoukouegno, F. Gaitho, G. T. Mola, M. Tsige, and G. Pellicane. Unravelling the surface composition of symmetric linear-cyclic polymer blends. *Fluid Phase Equilibria*, 441:33–42, 2017.
- [41] M. Jacobs, H. Liang, B. Pugnet, and A. V. Dobrynin. Molecular dynamics simulations of surface and interfacial tension of graft polymer melts. *Langmuir*, 34:12974–12981, 2018.
- [42] D. Prusty, V. Pryamitsyn, and M. O. d. l. Cruz. Thermodynamics of associative polymer blends. *Macromolecules*, 51:5918–5932, 2018.
- [43] T. Crisenza, H. Butt, K. Koynov, and R. Simonutti. Direct 3d visualization of the phase-separated morphology in chlorinated polyethylene/nylon terpolyamide based thermoplastic elastomers. *Macromolecular Rapid Communications*, 33:114–119, 2011.